Comparative photocatalytic performances towards acid yellow 17 (AY17) and direct blue 71 (DB71) degradation using Sn3O4 flower-like structure

by Bambang Yudono

Submission date: 16-Jan-2020 02:16PM (UTC+0700)
Submission ID: 1242553646
File name: t_blue_71_DB71_degradation_using_Sn3O4_flower-like_structure.pdf (1.61M)
Word count: 4409
Character count: 24311

Journal of Physics: Conference Series

Comparative photocatalytic performances towards acid yellow 17 (AY17) and direct blue 71 (DB71) degradation using Sn_3O_4 flower-like structure

Comparative photocatalytic performances towards acid yellow 17 (AY17) and direct blue 71 (DB71) degradation using Sn_3O_4 flower-like structure

A Huda[1], R Ichwani[2], C T Handoko[1], M D Bustan[3*], B Yudono[1], and F Gulo[1*]

[1] Program Studi Ilmu Lingkungan, Program Pascasarjana, Universitas Sriwijaya, Jalan Padang Selasa No. 524, Palembang 30121, Sumatera Selatan, Indonesia
[2] Department of Material Science and Engineering, Worcester Polytechnic Institute, Worcester-MA 01609, United State of America
[3] Program Studi Teknik Kimia, Fakultas Teknik, Universitas Sriwijaya, Jalan Palembang Prabumulih Km. 32 Indralaya Ogan Ilir 30862, Sumatera Selatan, Indonesia

*Corresponding author: djajashanta@yahoo.co.id; fgulo@unsri.ac.id

Abstract. Microsphere Sn_3O_4 flower-like structure has been successfully synthesized using a novel microwave-assisted hydrothermal method and comprehensively characterized by X-ray diffraction (XRD), field emission gun scanning electron microscope (FEG-SEM) and UV Vis spectrophotometer equipped with diffuse reflectance spectroscopy (UV-Vis DRS). In order to examine its photocatalytic performance, two synthetic azo-based dyes, acid yellow 17 (AY17) and direct blue 71 (DB71), have been used as organic pollutant models degraded under visible-light illumination. The results show that the negative charges of Sn_3O_4 produce higher efficiency photocatalytic activity on DB71 degradation compared to that on AY17 degradation. Further investigation has confirmed that the adsorption capacities played the main role in determining photocatalytic performance and differentiated the quantum yield of dye degradation. Moreover, the different adsorption capacities are generated by the formation of electrostatic interaction and repulsion between surface charge of Sn_3O_4 and dyes functional groups.

1. Introduction

Photocatalytic treatment is well known as a green technology process because of its potential to harvest and convert the photon energy to chemical energy and use it to degrade and mineralize most of organic pollutants [1]. Theoretically, the main mechanism of photocatalytic treatment began by activating the catalyst through light irradiation which has higher energies than the semiconductor band gap energy. The higher photon energies excite an electron from valence band to conduction band leaving a hole behind in valence band. The photo-generated hole has the electrophilic behavior which is naturally extract its surrounding electrons such as electrons of organic molecules, resulting in degradation or produce hydroxyl radical by oxidizing water molecules to directly oxidize the organic molecule.

Recently, studies on photocatalytic treatments have focused on designing the photocatalyst material which could effectively harvest the visible-light photon energy. It is based on the potential of

visible-light driven photocatalyst to harvest the visible-light photon energy from sunlight as the most abundant carbon and energy sources in the universe [2].

Many efforts have been conducted to explore the new functional metal oxides or semiconductor as photocatalytic materials [3]. The electronic properties of UV-based photocatalytic material have been also modified to harvest visible light spectrum instead of utilizing UV-light photon energy [4]. Flower-like structure of Sn_3O_4 is reported as a semiconductor which has photo-responses in UV and visible wavelength region [5]. Due to its relatively narrow band gap (2.5 to 2.9 eV), Sn_3O_4 can potentially utilize the energies of visible-light photon from sunlight [6]. In terms of applications, Sn_3O_4 has been widely reported to be used as a gas sensor [7], chemical sensor [8], anode material [9] and photocatalytic material [10]. To be more specific in photocatalytic oxidation, Sn_3O_4 has also been successfully used to oxidize the organic molecules such as methyl orange [10,11], rhodamine B [12] and 4-phenylazo-phenol [13].

Herein, the present study is designed to investigate the photocatalytic performance of as-prepared Sn_3O_4 to degrade the hydrophilic azo dyes of acid yellow 17 (AY17) and direct blue 71 (DB71). The study about photocatalytic oxidation of these azo dye is based on several facts about azo dyes. For example, azo dyes are the most used dyes worldwide, azo dyes consist of ~80% azo chromogen and around 52-57% of azo dye groups which is chemically stable and non-biodegradable compound [14]. The successful degradation of those dyes using Sn_3O_4 in a visible light region could offer an effective way of textile dye wastewater treatments. The effect of adsorption process and dyes complexity in the photocatalytic performance of Sn_3O_4 are comprehensively investigated. Moreover, the results are expected to give some point of views of some main parameters which play important roles in determining the photocatalytic performance of Sn_3O_4.

2. Experimental Section

2.1. Preparation and characterization of Sn_3O_4

Sn_3O_4 used in this study was synthesized through a microwave-assisted hydrothermal method by dissolving 6 mmol of SnF_2 (Sigma-Aldrich, ≥99.9% of purity) as the precursor in the mixture solvent of absolute ethanol and distilled water with the volume ratio of 1:2. The suspended solution was slowly stirred for 30 minutes in room temperature. The solution pH was carefully adjusted to 6 by dropping 1 mol L^{-1} sodium hydroxide (NaOH) solution and transferred into a Teflon–lined autoclave. The synthesis process was hydrothermally heated at 150°C for 120 minutes with a heating rate of 10°C and then naturally cooled down to room temperature. The Sn_3O_4 powder was obtained by centrifugation at 10.000 rpm and cleaned with distilled water for several times and finally with absolute ethanol. The powder was dried at 70°C overnight before characterization.

The as-prepared catalyst Sn_3O_4 was characterized using X-ray diffractometer (XRD) (Rigaku, model D-Max 2500) using Cu-Kα radiation to determine the crystal structure, phase and composition. The catalyst surface morphology was confirmed by field-emission gun scanning electron microscopy (FEG-SEM) (JEOL, model JSM-7500F). The photoresponse properties of catalyst were measured using Ultraviolet-visible spectrophotometer supported diffuse reflectance spectroscopy (Shimadzu UV-2600 series). In addition, the surface charge of catalyst as a function of pH was investigated by Zeta analyzer (Malvern Zetasizer Nano Series).

2.2. Photocatalytic test

The photocatalytic activities of Sn_3O_4 were evaluated using a suspended system (Figure 1). 25 mg of as-prepared Sn_3O_4 were suspended onto 10 ppm dye solution in 250 mL of distilled water. Prior to illumination, the suspended solution (catalyst+dye solution) was stirred in dark condition for 30 minutes to study the adsorption capacities of Sn_3O_4. After 30 minutes, the suspended solution was illuminated with 125 W High-Pressure Hg-Lamp (Osram) equipped with a cylindrical glass tube to ensure that the irradiation was only irradiated by a visible light source (>390 nm) [15]. The photocatalytic activities were determined by measuring the discoloration performance as a function of irradiation time at the maximum wavelength of dye solution using UV-Vis spectrophotometer (Philips

US5300). To study the effect of light irradiation to dyes the discoloration, the photolysis experiments were conducted using a similar procedure and condition in the presence of catalyst [16].

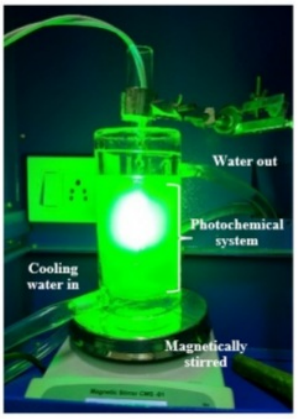

Figure 1. Experiment set up of photocatalytic test.

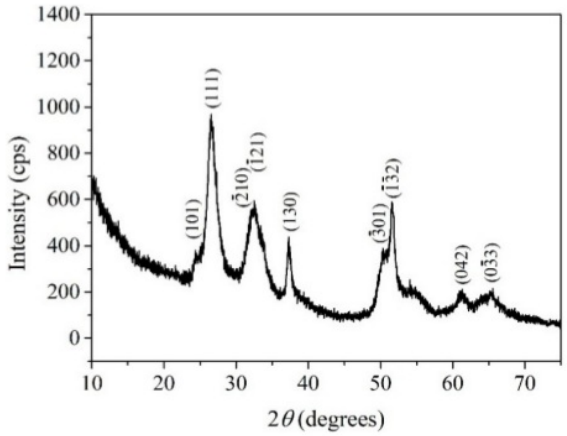

Figure 2. XRD patterns of as-prepared Sn_3O_4 flower-like structure

3. Results and Discussion

3.1. Material characterization

The XRD pattern in Figure 2 proves that all as-prepared catalyst powder corresponds to triclinic Sn_3O_4 material (JCPDS No. 16.0737). The peaks of Sn_3O_4 has been identified at 27.36°, 32.32°, 33.04°, 37.47°, 50.42°, 52.73°, 61.00° and 66.13°. Inside limitation of XRD technique, there is no residual contaminants or impurities such as SnO, SnO_2 or the other intermediate phase observed which indicates high efficiency of microwave-assisted hydrothermal method.

In order to study the catalyst morphologies, Field Emission Gun Scanning Electron Microscopy (FEG-SEM) were employed. Figure 3 shows typical images of Sn_3O_4 flower-like structure which is in accordance with the previous reported work [17]. The high magnification image shows that flower-like structure were self-assembled by thin nano-sheets with sharp edges and smooth surfaces. The flower-like sphere presents the diameter distribution of 0.2 – 0.7 µm and the nano-sheets thickness of 5-10 nm.

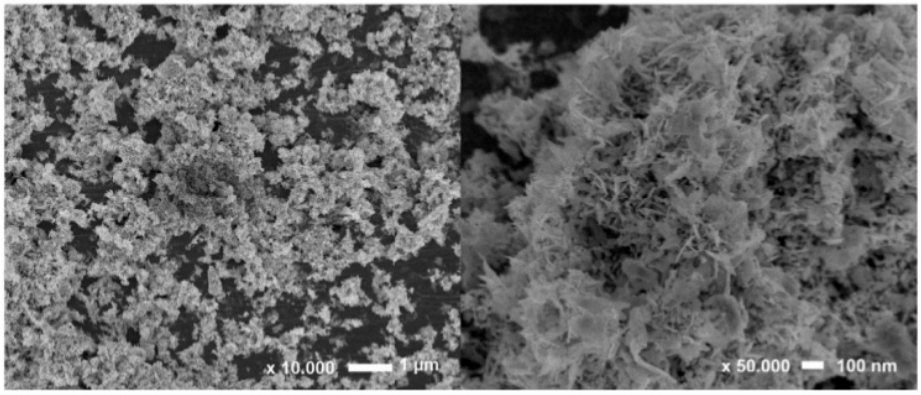

Figure 3. SEM images of as-prepared Sn_3O_4 with different magnifications

The optical properties of Sn_3O_4 were investigated using a UV-visible spectrophotometer equipped with diffuse reflectance spectroscopy (UV-VIS DRS). As shown in Figure 4, Sn_3O_4 presented the photoabsorption ability as % reflectance from UV-light to visible light wavelength region from 400 nm to 550 nm. However, the wavelength above 550 nm will not activate Sn_3O_4 as photocatalytic material. The further investigation using Kubleka-Munk approach is used to estimate the optical band gap of Sn_3O_4 and provides the minimum light irradiation wavelength to activate the catalyst [18].

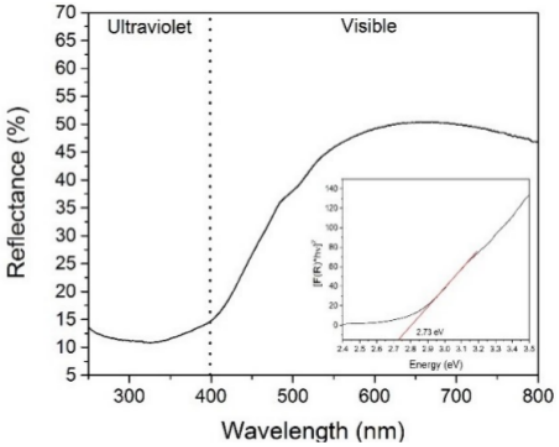

Figure 4. UV-VIS DRS spectra of as-prepared Sn_3O_4. Inset images shows the plotting of K-M function vs bandgap energy.

The calculation of optical band gap was conducted by plotting the Kubelka-Munk function multiplied by energy [F(R)*hv] versus photon energy in eV shown in inset of Figure 4. The band gap energy was evaluated as around 2.73 eV. Furthermore, the minimum energy band gap was determined by substituting the calculated-band gap energy (eV) based on equation (1). As a result, the minimum band gap to activate the catalyst was obtained in 455 nm meaning longer wavelength (λ>455 nm) radiation will not excite the electron of catalyst.

$$E\ (eV) = \frac{1240}{\lambda\ (nm)} \quad (1)$$

3.2. Photocatalytic activity

The study of photocatalytic activity began by investigating the adsorption-desorption capacities of catalyst. The adsorption-desorption test was conducted by directly mixing the catalyst and dye solution (AY17 and DB71) in a dark condition. The result showed that Sn_3O_4 exhibited the different adsorption capacities between both dyes, in which the adsorption capacity through DB71 was higher compared to that on AY17 adsorption. It is expected that the difference of adsorption capacities was influenced by the interaction between the catalyst surface and the functional group of dyes. In this experiment, all system used pH 5-6 as a natural pH of dyes in H_2O, indicating Sn_3O_4 has a negative surface charge (pH_{zpc} = 2-3) [19]. Furthermore, the lower adsorption-desorption capacity of AY17 removal is affected by the formation of electrostatic repulsion between the anionic functional group of AY17 such as Cl^- and OH^- and the negatively charged of catalyst surface. The phenomenon of electronic repulsion and interaction was supported by Ratnamala, M (2017) who reported that the negatively charged surface site on the adsorbent did not favor the adsorption of anionic dyes due to electrostatic repulsion [20]. Compared to the AY17 adsorption, the color removal of DB71 through adsorption process showed higher percentages because DB71 had the cationic functional groups such as NH_2 and three azo groups which easily formed the electrostatic interaction with catalyst surface resulting in the high adsorption removal capacities. Moreover, the adsorption-desorption process is seen as the initial stage of photocatalytic degradation and assumed as an important parameter before measuring the photocatalytic performance.

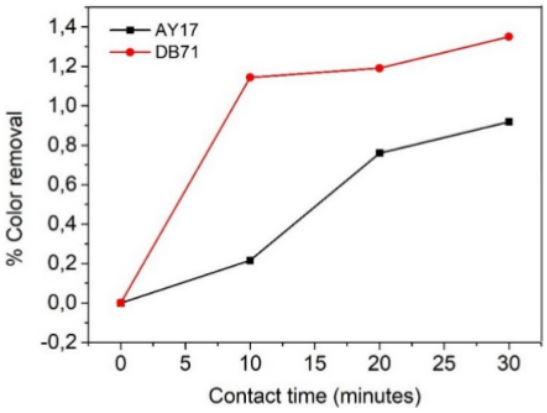

Figure 5. Percentages of color removal during adsorption-desorption process using Sn_3O_4

After measuring the adsorption capacity, the photolysis test has been done by irradiating both dyes using 125W Hg-lamp in the absence of Sn_3O_4. The result showed that approximately 14% of AY17 and 5% of DB71 were decomposed after 30 minutes of photolysis test indicating that DB71 is relatively more stable under light irradiation than AY17. The light stability of both dyes was differentiated by the numbers of azo group contained in the dye chemical structure. In the photolysis test, the π-bonds of azo group easily abstracted the surrounding hydrogen atom, resulting in the breakage of azo group molecules [21]. The breakage of azo group as chromophore group gave the photoresponse as decreasing color adsorption. However, the high number of azo group of DB71 generates a conjugated system which exhibits electron resonance flowing from one azo dye to the other azo functional group, resulting in high stability dyes through light irradiation [22]. Thus, the DB71 has lower color removal percentages during photolysis compared to that on AY17. Figure 6 shows the photolysis result of AY17 and DB71.

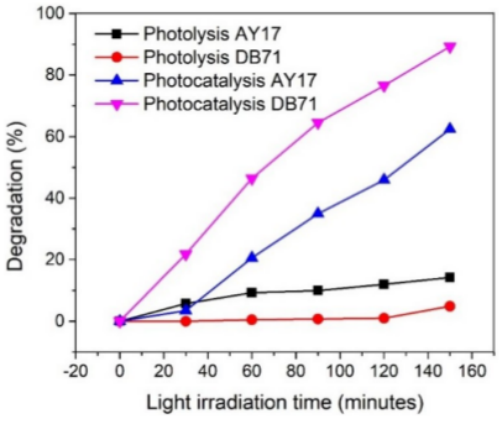

Figure 6. Photodegradation of AY17 and DB71 in photolysis and photocatalysis process

The study was continued through photocatalytic experiment. Figure 6 showed that the percentages of DB71 and AY17 degradation slightly increased reaching 89.209% and 62.418%, respectively after switching on the light source. It is interesting that the degradation of triazo dye group of DB71 which had more molecular complexity exhibited higher percentages of degradation than monoazo AY17 degradation. Furthermore, the different photocatalytic performances between both dyes were assumed by the contribution of adsorption capacities as the initial stage of photocatalytic degradation. The adsorption process determines the possibilities of contact between the active surface of catalyst and the dyes. The electrostatic interaction provides the interfacial charge between the active site of Sn_3O_4 and dyes resulting in the spontaneous reaction. This phenomenon facilitates higher possibilities of contact

between the active site of Sn_3O_4 and dyes, indicating higher photocatalytic oxidation yield. On the other hand, the presence of a carbonyl group in DB71 structure possibly enhanced the photocatalytic performance due to easily reacting H^+ and carbonyl group via photo Kolbe reaction resulting in the improvement of the photocatalytic degradation [23].

However, the electrostatic repulsion occurred during AY17 degradation generates less contact between catalyst and dyes and initiate the phenomenon of electron-hole recombination. The recombination process is generated because the photogenerated-electron do not spontaneous contact with the dyes, resulting in falling the electron from the conduction band to valence band. These condition makes the empty active site of Sn_3O and generates low photocatalytic performance. Moreover, the result becomes the important information that shows the role of adsorption process in the photocatalytic reaction. However, the results exhibited that the pollutant complexity or molecular complexity does not give a significant effect in determining of photocatalytic activity.

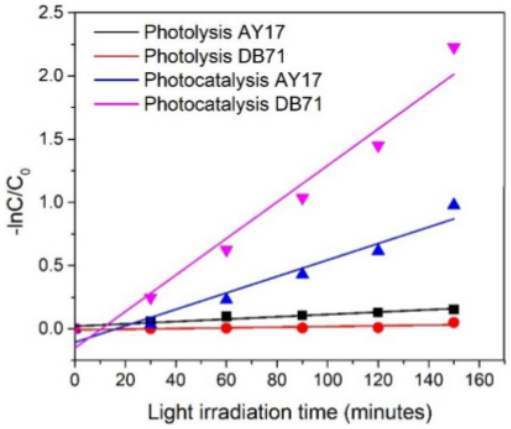

Figure 7. The first-order kinetics in the azo dyes degradation through photolytic and photocatalytic reactions.

The photodegradation has been further studied by determining the kinetics constant of each process. Before measuring the kinetic rates of photocatalytic degradation, it should be well explained that the photocatalytic reaction is a reaction conducted by the light-absorbing species in which light becomes the key parameter to initiate the reaction. Thus, there is no reaction without light irradiation even the catalyst has high purity, excellent properties and photo-response. The environmental parameters such as temperature and pressure which commonly influence the kinetic rate of reaction could not contribute to the photocatalytic degradation [24]. In general, as a homogeneous reaction, a reaction could be written as:

$$S \rightarrow P \tag{2}$$

where in thermal reaction, the disappearance rate of substrates (S) to produce products (P) as a function of reaction time could determine the kinetic rate of reaction (2). The detail expression to determine the kinetic rate (k) is shown below.

$$-\frac{d[S]}{dt} = k\ x\ [S] \tag{3}$$

$$-\frac{d[S]}{[S]} = k\ x\ dt \tag{4}$$

Integration equation (4) generates equation (5)

$$\frac{\ln[S]}{[S_0]} = -k\ x\ t \tag{5}$$

By plotting the $\ln[S]/[S_0]$ conducted by controlling the dyes absorbance at absorption maximum wavelength of 405 nm and 588 nm for AY17 and DB71, respectively, versus time, the linear plot

could be determined as the first order kinetic rate of equation (2). In photochemical reaction (equation 6), light irradiation involves into the reaction and determines the kinetic rate of reaction. The kinetic constant rate in the photochemical reaction is given by some equation below [24].

$$S + h\nu \rightarrow P \tag{6}$$

$$-\frac{d[S]}{dt} = \emptyset(\lambda)s \; x \; I_a \tag{7}$$

Substitute –d[S]/dt in equation (3) generate equation (8).

$$k * [S] = \emptyset(\lambda)s \; x \; I_a \tag{8}$$

where k is the first order kinetic rate constant, *Ø(λ)s* is the quantum yield conducted in the reaction at the wavelength (λ) which generate the disappearance of substrate, and I_a is the number of a photon of wavelength λ absorbed per second and volume (photon flux).

Utilizing the equation 8 result that quantum yield becomes the key parameter to be compared during the photocatalytic process in which followed the basic assumption in photocatalytic degradation, Quantum yield is determined as

$$Quantum\ yield\ (\emptyset) = \frac{number\ \ of\ molecule\ \ degrade\ \ per\ area\ \ per\ second}{number\ \ of\ incident\ \ photon\ per\ area\ \ per\ second} \tag{9}$$

Rearrangement equation (8) represents the equation (9) and obtains the equation (10) in which the number of molecule degrade equals to the first order kinetic rate constant and the number of incident photon is the number of photon flux.

$$Quantum\ yield\ (\emptyset) = \frac{k\ [S]}{I_a} \tag{10}$$

The photon flux could be calculated using the equation (11) given below.

$$I_a = \frac{Power\ \ density\ \left(\frac{W}{m^2}\right) * \lambda}{Energy\ \ (eV)} \tag{11}$$

Rearrangement equation (10) with equation (11) generates the equation (12).

$$Quantum\ yield\ (\emptyset) = \frac{k\ [S] * Energy\ \ (eV)}{Power\ \ density\ \left(\frac{W}{m^2}\right) * \lambda} \tag{12}$$

where the number of molecule degrade equals to the first order kinetic rate constant of photocatalytic degradation (second^{-1}), and the number of incident photon is the photon flux irradiated during the photochemical reaction at the minimum wavelength (λ) to activate semiconductor. As the result, Table 1 shows the first order kinetic rate and the quantum yield of each photodegradation process.

Table 1. The first order kinetic rate constant and decay quantum yield of AY17 and DB71 in photolytic and photocatalytic degradations.

Conditions	kinetic rate constant (min^{-1})	Quantum yield (Ø)
Photolysis AY17	9.32 x 10^{-4}	3.52 x 10^{-6}
Photolysis DB71	2.67 x 10^{-4}	1.01 x 10^{-6}
Photocatalysis AY17	6.5 x 10^{-3}	2.45 x 10^{-5}
Photocatalysis DB71	4.6 x 10^{-2}	1.74 x 10^{-4}

Table 1 shows that the quantum yield of photolytic degradation of both dyes was relatively very low as the presence of catalyst increases the efficiencies. The result of quantum yield measurement also indicates that the quantum yield is correlated with their kinetic constant of each process. The improvement of quantum yield could be contributed by the highly oxidative agent from activated-catalyst which help to degrade the dyes. As the catalyst receives an exposure of photon energy from the light source, it absorbs the photon energy (hv) and promotes an electron from valence band to conduction band, leaving photogenerated holes behind in valence band [25]. The photogenerated holes

with its electrophilic behavior could extract electrons from its surrounding which has a high number of electron such as azo group of dye. The electron can break down the π-bond of azo group resulting in the degradation of dyes. The photodegradation was not only breaking down the bond but also breaking other organic molecules through some process such as de-ethylation or de-methylation which produces benign products, ideally CO_2, as the result of complete oxidation. On the other hand for photolytic case, the degradation was generated by the light irradiation which potentially breaks the bond of chromophore group through abstracting the surrounding hydrogen. All degradations could happen only if the illuminated-photon energies are higher than the binding energy of dye molecules. In this study, it can be assumed that only the light which has the wavelength less than 455 nm could be used to degrade the dyes for calculating in the quantum yield.

4. Conclusion

In summary, the study proved that single flower-like structure of Sn_3O_4 has visible light photoresponse with calculated band gap of 2.73 eV. The photocatalytic results shows that Sn_3O_4 effectively degrades DB71 dye compared to that on AY17 dye. The further investigation successfully found that presence of electrostatic interaction and repulsion between the Sn_3O_4 surface and the functional group of AY17 and DB71 dyes is attributed to the different percentages of photodegradation of both dyes. The results also indicate that the molecular complexity do not affect the performance of Sn_3O_4, whereas the adsorption process plays the crucial role in determining the efficiency of photocatalytic degradation.

Acknowledgment

The authors thank the Ministry of Research, Technology, and Higher Education of the Republic of Indonesia for financial support Grant no. 0058/E4.4/N9/SB3.LP2M.PT/2018. Authors also acknowledge Prof. M. O. Orlandi, Prof. M. V. B. Zanoni, P. H. Suman, Ph.D., L. D.M. Torquato, Ph.D from Institute of Chemistry, Sao Paulo State University, Brasil for supporting the interpretation and discussion about the preparation and application of tin oxide-based material.

References

[1] Hernández-Ramírez A and Medina-Ramírez I 2015 *Photocatalytic Semiconductors* (Cham: Springer International Publishing)
[2] Pan H 2016 Principles on design and fabrication of nanomaterials as photocatalysts for water-splitting *Renew Sust Energ Rev* **57** 584–601
[3] Huda A, Handoko C T, Bustan M D, Yudono B and Gulo F 2018 New route in the synthesis of Tin(II) oxide micro-sheets and its thermal transformation *Mater. Lett.* **211** 293–5
[4] Huda A, Ichwani R, Handoko C T, Yudono B, Bustan M D and Gulo F 2018 Enhancing the visible-light photoresponse of SnO and SnO_2 through the heterostructure formation using one-step hydrothermal route *Mater. Lett.* **238** 264-266
[5] Shvalagin V V, Grodzyuk G Y, Shvets A V, Granchak V M, Lavorik S R and Skorik N A 2015 Photochemical Reduction of Silver and Tetrachloroaurate Ions on the Surface of Nanostructured Sn_3O_4 Under the Influence of Visible Light *Theor. Exp. Chem.* **51** 177–82
[6] Manikandan M, Tanabe T, Li P, Ueda S, Ramesh G V, Kodiyath R, Wang J, Hara T, Dakshanamoorthy A, Ishihara S, Ariga K, Ye J, Umezawa N and Abe H 2014 Photocatalytic Water Splitting under Visible Light by Mixed-Valence Sn_3O_4 *ACS Appl Mater Inter* **6** 3790–3793
[7] Suman P H, Felix A A, Tuller H L, Varela J A and Orlandi M O 2015 Comparative gas sensor response of SnO_2, SnO and Sn_3O_4 nanobelts to NO_2 and potential interferents *Sensors Actuators B Chem.* **208** 122–127
[8] Li X, Wang F, Tu J, Shah H U, Hu J, Li Y, Lu Y and Xu M 2015 Synthesis and Ethanol Sensing Properties of Novel Hierarchical Sn_3O_4 Nanoflowers *J Nanomater* **2015** 1–7
[9] Chen X, Huang Y, Zhang K, Feng X and Wei C 2017 Novel hierarchical flowers-like Sn_3O_4 firstly used as anode materials for lithium ion batteries *J. Alloys Compd.* **690** 765–770
[10] Chen G, Ji S, Sang Y, Chang S, Wang Y, Hao P, Claverie J, Liu H and Yu G 2015 Synthesis of scaly Sn_3O_4/TiO_2 nanobelt heterostructures for enhanced UV-visible light photocatalytic

activity *Nanoscale* **7** 3117–25
[11] Song H, Son S-Y, Kim S K and Jung G Y 2015 A facile synthesis of hierarchical Sn_3O_4 nanostructures in an acidic aqueous solution and their strong visible-light-driven photocatalytic activity *Nano Res* **8** 3553–3561
[12] Xia W, Wang H, Zeng X, Han J, Zhu J, Zhou M and Wu S 2014 High-efficiency photocatalytic activity of type II SnO/Sn_3O_4 heterostructures via interfacial charge transfer *CrystEngComm* **16** 6841
[13] He Y, Li D, Chen J, Shao Y, Xian J, Zheng X and Wang P 2014 Sn_3O_4 : a novel heterovalent-tin photocatalyst with hierarchical 3D nanostructures under visible light *RSC Adv.* **4** 1266–1269
[14] Ertugay N and Acar F N 2017 Removal of COD and color from Direct Blue 71 azo dye wastewater by Fenton's oxidation: Kinetic study *Arab. J. Chem.* **10** S1158–63
[15] Dunnill C W 2014 UV Blocking Glass: Low Cost Filters for Visible Light Photocatalytic Assessment *Int. J. Photoenergy* **2014** 1–5
[16] Cardoso J C, Bessegato G G and Boldrin Zanoni M V 2016 Efficiency comparison of ozonation, photolysis, photocatalysis and photoelectrocatalysis methods in real textile wastewater decolorization *Water Res.* **98** 39–46
[17] Chen X, Huang Y, Li T, Wei C, Yan J and Feng X 2017 Self-assembly of novel hierarchical flowers-like Sn_3O_4 decorated on 2D graphene nanosheets hybrid as high-performance anode materials for LIBs *Appl. Surf. Sci.* **405** 13–9
[18] Goodall J B M, Kellici S, Illsley D, Lines R, Knowles J C and Darr J A 2014 Optical and photocatalytic behaviours of nanoparticles in the Ti–Zn–O binary system *RSC Adv.* **4** 31799
[19] Huda A, Mahendra I P, Ichwani R, Handoko C T, Ngoc H M, Yudono B, Bustan M D and Gulo F 2019 High Efficient Visible-light activated Photocatalytic semiconductor SnO_2/Sn_3O_4 heterostructure in Direct blue 71 (DB71) degradation **12** 308–318
[20] Ratnamala M, Rahul M, Sameer S, Vaani M, Omkar and Devdatt T 2017 Column Studies for Removal of Acid Yellow Dye 17 from Synthetic Water Using Activated Saw Dust *Asian J. Chem.* **29** 191–5
[21] Tsui S and Chu W 2001 Quantum yield study of the photodegradation of hydrophobic dyes in the presence of acetone sensitizer *Chemosphere* **44** 17–22
[22] IARC Monographs Working Group on the Evaluation of Carcinogenic Risks to Humans 2010 Some aromatic amines, organic dyes, and related exposures. *IARC Monogr. Eval. Carcinog. Risks Hum.*
[23] Lachheb H, Puzenat E, Houas A, Ksibi M, Elaloui E, Guillard C and Herrmann J-M 2002 Photocatalytic degradation of various types of dyes (Alizarin S, Crocein Orange G, Methyl Red, Congo Red, Methylene Blue) in water by UV-irradiated titania *Appl. Catal. B Environ.* **39** 75–90
[24] Kisch H and Bahnemann D 2015 Best Practice in Photocatalysis: Comparing Rates or Apparent Quantum Yields? *J. Phys. Chem. Lett.* **6** 1907–10
[25] Ajmal A, Majeed I, Malik R N, Idriss H and Nadeem M A 2014 Principles and mechanisms of photocatalytic dye degradation on TiO_2 based photocatalysts: a comparative overview *RSC Adv.* **4** 37003–37026

Comparative photocatalytic performances towards acid yellow 17 (AY17) and direct blue 71 (DB71) degradation using Sn3O4 flower-like structure

ORIGINALITY REPORT

13%	10%	13%	11%
SIMILARITY INDEX	INTERNET SOURCES	PUBLICATIONS	STUDENT PAPERS

PRIMARY SOURCES

1	Submitted to Udayana University Student Paper	6%
2	rasayanjournal.co.in Internet Source	2%
3	eprints.whiterose.ac.uk Internet Source	1%
4	A. Huda, P.H. Suman, L.D.M. Torquato, Bianca F. Silva, C.T. Handoko, F. Gulo, M.V.B. Zanoni, M.O. Orlandi. "Visible light-driven photoelectrocatalytic degradation of acid yellow 17 using Sn3O4 flower-like thin films supported on Ti substrate (Sn3O4/TiO2/Ti)", Journal of Photochemistry and Photobiology A: Chemistry, 2019 Publication	1%
5	sintadev.ristekdikti.go.id Internet Source	1%

6	eprints.unsri.ac.id Internet Source	1%
7	Klito C. Petallidou, Angelos M. Efstathiou. "Low-temperature water-gas shift on Pt/Ce1−xLaxO2−δ: Effect of Ce/La ratio", Applied Catalysis B: Environmental, 2013 Publication	1%

Exclude quotes	On	Exclude matches	< 1%
Exclude bibliography	On		